Perovskite-based Catalysts for Direct Ethanol Fuel Cells

Aidong Lan and Alexander S. Mukasyan*

Department of Chemical and Biomolecular Engineering, Center for Molecularly Engineered Materials,
University of Notre Dame, Notre Dame, IN 46556, USA

Abstracts

Utilizing a screening strategy featuring energy efficient and rapid solution combustion (SC) synthesis technique, and the high throughput NuVant system, a library of conductive perovskites was synthesized and tested as anode electrode in the direct ethanol fuel cell (DEFC) conditions. It was found that a variety of Ru-based perovskites showed considerable electro-catalytic activity for ethanol oxidation. Further, it was demonstrated that the perovskite-platinum catalysts with low noble metal loading prepared directly in by SC method exhibit comparable performance with standard Pt-Ru alloy.

Introduction

Direct alcohol proton exchange membrane fuel cells (PEMFC) are considered as an advanced source of energy for a variety of applications, particularly for the electric vehicles [1,2]. Among different alcohols a methanol because of its low cost and easiness of storage is widely suggested as a primary fuel for PEMFC [3,4]. However, the aspect of the methanol toxicity remains crucial [5]. Ethanol is an alternative low toxic fuel, which can be attractive for various usages. Having higher cost than methanol, ethanol possesses additional advantage, *i.e.* its availability from a broad variety of biomass products.

The complete electro-oxidation of ethanol at anode involves 12 electrons per molecule as follows: $CH_3CH_2OH + 3H_2O \rightarrow 2CO_2 + 12H^+ + 12e^-$. In the dissociation process of ethanol at anode, different intermediate chemisorbed species are produced, including acetaldehyde and acetic acid. Carbon monoxide (CO) is also formed and considered to be a poisoning agent because it blocks the electro-catalytic active sites and hence reduces the overall performance of cell [6,7]. In addition, the reaction mechanism involves the participation of water, or of its adsorption residue, so that a good electrocatalyst must activate both the chemisorption of alcohol and the water molecules. Finally, ethanol electro-oxidation to carbon di-oxide requires the cleavage of the C–C bond. Above complexities make ethanol oxidation more difficult than that of methanol [3,8]. Thus for effective operation of direct ethanol fuel cells (DEFCs) it is even more critical to develop an inexpensive poly functional catalyst with appropriate solid state, surface, and morphological properties [5,9,10].

So far platinum-based materials have been studied as catalysts for DEFCs application [*cf.* 5]. Indeed, Pt is the only known active and stable noble metal in acid environment (proton exchange membrane). The platinum alloys are believed to be effective electrocatalysts for ethanol oxidation. One of the promising candidates is Pt-Sn alloy, which allows the ethanol oxidation at lower potential than for pure platinum [*cf.* 11,12]. However, Pt-Ru standard possesses current densities which are higher than for Pt-Sn alloy. For this reason and also accounting our experience of working with Pt-Ru catalyst this alloy was used for rating of electro-catalytic activities of perovskite based compositions.

In this work we suggest a different approach for developing of the effective multifunctional catalysts for DEFCs. As noted above, the successful strategy of electro-catalyst design for ethanol oxidation should consider two important aspects: (i) promoting water and ethanol adsorption; (ii) facilitating oxidation of intermediate products and CO. Thus it is proposed that mixed conductor complex oxides, some of which are known as excellent water adsorbents and catalysts for CO oxidation [13], could be the alternative materials for DEFC application.

*corresponding author. E-mail: amoukasi@nd.edu

More specifically, it is known that some perovskites (ABO_3) are electronically conductive and also possess excellent proton transport property [14]. In addition, the surfaces of perovskite compounds are acidic, and hence, they are stable and active in the strong acid environment. The vast applications of perovskites for reforming of hydrocarbon suggest that such materials should have better tolerance towards oxidation of reactive sites than Pt alloys [13].

Thus it is a logical approach to develop a multi-functional catalyst for DEFCs application based on such perovskite structures. In the current work, a numerous perovskite compositions were synthesized by using solution combustion synthesis approach [cf. 15-17]. The electro-catalytic performances of the obtained materials were tested in the fuel cell conditions by using electrochemical screening system NuVant 100P [cf. 18,19]. It was shown that optimized perovskite-based materials are promising candidates as anode electro-catalysts in DEFC.

Experimental Procedure

Synthesis of the Catalyst

Solution combustion synthesis is an attractive technique for the production of different oxides, including ferrites, perovskites, and zirconia [cf. 20-22]. It involves a self-sustained reaction between an oxidizer (e.g. metal nitrate) and a fuel (e.g. glycine, hydrazine). In these work the metal nitrates $Me(NO_3)_x$ (where Me = Ba, Ca, Sr, La,) as a oxidizers and glycine $C_2H_5NO_2$, as a fuel were used to synthesize different catalysts. Ruthenium Nitrosyl Nitrate solution was used to prepare Ru-based perovskites. Some properties of the precursors are shown in Table 1.

Under equilibrium conditions, in general the reactions in these systems can be represented as follows:

$$Me^v(NO_3)_v + (\frac{5}{9} v \cdot \phi) \, CH_2NH_2CO_2H +$$

$$+ v \cdot \frac{5}{4} (\phi - 1)O_2 \Rightarrow MeO_{v/2}^{(s)} + (\frac{10}{9} v \cdot \phi)CO_2^{(g)} +$$

$$+ \frac{25}{18} \phi \, H_2O^{(g)} + v \cdot (\phi + 1)/2 \, N_2^{(g)}$$
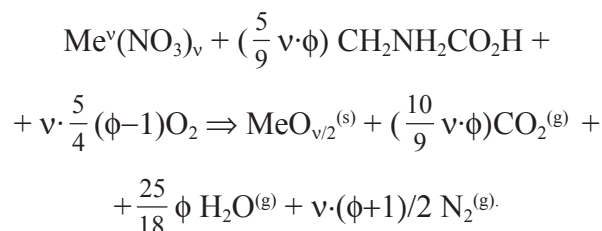
where Me^v is a metal with v – valence, ϕ is a fuel to oxidizer ratio, $\phi = 1$ means that the initial mixture does not require atmospheric oxygen for complete oxidation of fuel, while $\phi > 1$ (< 1) implies fuel-rich (lean) conditions. For example, during the synthesis of the $LaRuO_3$ perovskite the following stoichiometric ($\phi = 1$) reaction occurs:

$$La(NO_3)_3 + Ru(NO)(NO_3)_3 +$$
$$+ 32/5 \cdot C_2H_5NO_2 \Rightarrow LaRuO_3 + 32/5 \cdot CO_2\uparrow_g +$$
$$+ 16H_2O\uparrow_g + 67/10 \cdot N_2\uparrow_g$$
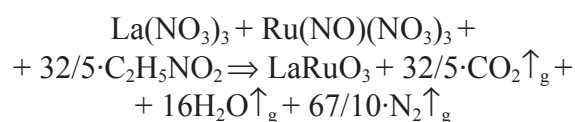
While different reaction modes [23-25], including Volume Combustion Synthesis (VCS), self-propagating Sol-Gel Combustion (SGC), and Impregnated Support Combustion (ISC) exist, in this work we utilized conventional VCS approach. First, reactants are dissolved in water (see Table 1) and the obtained solution is thoroughly mixed to reach essential molecular level of homogenization for the reaction medium. After preheating to its boiling point (100°C) water evaporates and further heating leads to solution self-ignition at some temperature (T_{ig}), which varies for different system (e.g. ~ 130°C for $LaRuO_3$ and 250°C for $SrRuO_3$). After ignition the temperature rises rapidly (up to 10^3 °C·s^{-1}) to values as high as 1500°C. This high temperature be accompanied by intensive gasification (CO_2, N_2, steam) during short time pe-

Table 1
Some Properties of the Precursors

Precursor	Molecular weight	Solubility in 100 g of water 20°C	Melting Point, °C	Vendor, purity
$La(NO_3)_3 \, 6H_2O$	433.06	> 10%	45 (b.p. 126)	Alfa Aesar, 95%
$Ba(NO_3)_2$	261.34	8.7 g	592 (decomp.)	Alfa Aesar, 99%
$Ca(NO_3)_2 \, 4H_2O$	236.15	121	45	Alfa Aesar, 98%
$Sr(NO_3)_2$	212.00	71	570 (b.p. 645)	Alfa Aesar, 100%
$Ru(NO)(NO_3)_3$	317.09	miscible	b.p. 1100	Alfa Aesar, 1.5 wt.% Ru
$CH_2NH_2CO_2H$	75.07	25	182 (decomp. 238)	Alfa Aesar, 98%

riod (0.1-1 s) converts the initial solution to fine well-crystalline powder of desired composition.

Beside pure perovskites the design of multifunctional catalyst involves preparation of perovskite-platinum composite. In previous work [24] we used two approaches for Pt incorporation into oxide-based catalyst, *i.e.* "internally" during solution combustion (SC) synthesis or "externally" during ink preparation. It was shown that internal method, where complex-catalysts were synthesized by addition of Pt containing reagent (*e.g.* tetra-ammine-platinum nitrate) into initial metal nitrate + glycine solution, leads to superior electro-catalytic activity of produced compositions. Thus all results discussed below were obtained on oxide-metal catalysts synthesized by internal SC method.

The products phase compositions and crystallinity were determined by using X_1 advanced diffraction system (Scintag Inc.). The specific surface area (BET) of powders was measured by Autosorb 1C (Quantchrome Instruments, USA) apparatus.

Catalyst Screening

The electrochemical screening system NuVant 100P was developed by Liu & Smotkin [18]. It consists of electronically insulating block with array of fuel cells that accommodates 25 independent graphite sensor electrodes laid out in a 5×5 matrix. Each sensor is contacted the non-catalyzed face of the gas diffusion layer (GDL) disk, the catalyzed side of which contacts the Nafion 117 (DuPont Nafion Products, Fayetteville, NC) membrane electrolyte. Serial of flow fields machined on a ceramic fuel cell block permits delivery of fuel (liquid or gas) to each electrode. A computer controlled array potentiostat was used to condition the array and acquire the polarization curves (see Ref. 18 for details).

Anode and cathode catalyst inks are prepared by dispersion of the corresponding catalysts powders in solubilized Nafion solution (Aldrich, Milwaukee, WI), as described elsewhere [26]. Array GDLs for catalyst candidates are prepared by evenly coating GDL carbon fiber paper (Toray paper, E-TEK, TGPH-60) and then punching out 0.713 cm² disks. Typically six replicate samples for each of the four catalyst compositions and one blank sample disk were randomly positioned in the array. The loading for perovskite catalysts was ~ 6 mg/cm², while for standard Pt or Pt-Ru catalysts ~ 4 mg/cm² (see Table 2). The Pt loading for the common counter/reference electrode was

1 mg/cm². The counter/reference electrode was hot pressed (160°C at 1800 lb-force for 5 min) onto Nafion 117 membrane. The 25 working electrodes were hot pressed (160°C at 1000 lb-force for 5 min) onto the other side of the Nafion sheet, thus creating Membrane Electrode Assembly (MEA).

A NuVant Systems NUV100P was used to test the catalysts. The array fuel cell was conditioned by passing wet hydrogen through both sides of the MEA at 60°C for 12 hrs while cycling between 0-0.2 V *vs.* the counter hydrogen electrode. The anode stream was then switched to ethanol (1 M, 8 mL/min) and the array of fuel cells was conditioned by cycling between 0 and 0.7 V until reaching steady-state performance. The set of polarization curves were then simultaneously obtained by potential sweeps (cyclic voltammetry) from 0 to 0.8 V. Note that potential was taken with respect to dynamic hydrogen electrode (DHE). The specific feature of this work is that for study of the long-term catalysts activity the potentiostatic (at constant potential between 0.4-0.8 V) measurements were also conducted for the duration of several hours.

Results and Discussions

Synthesis and Microstructural Characterization

On the initial stage of the research the main criteria for selection of the material compositions was their electro-conductivity. It is known that such families as $ARuO_3$ and $A'FeO_3$ (where A = Ba, Ca, Sr, La, A' =

Table 2
Some Characteristics of the Catalysts

Composition	Catalyst Loading, mg/cm²	Actual Pt Loading, mg/cm²	Surface Area, BET, m²/g
$SrFeO_3$	5.7	0.00	1.5
$BaRuO_3$	5.6	0.00	1.5
$CaRuO_3$	3.0	0.00	18.4
$SrRuO_3$	5.9	0.00	4.0
$SrRuO_3$ + 5 wt.% Pt	5.8	0.29	3.1
$LaRuO_3$	5.9	0.00	8.5
$LaRuO_3$ + 5 wt.% Pt	6.9	0.34	4.3
Pt-black	3.0	3.0	30.0
Pt/Ru alloy	4.7	3.10	62.0

Sr, Ca) are good conductors [27]. An additional incentive for choice of ruthenium as a B site element correlates with reported Ru catalytic activity for the methanol oxidation [*cf.* 2], while the selection of iron is partially favored by its excellent reactivity in the combustion wave [*cf.* 15]. A library of different perovskites families was synthesized by VCS mode of solution combustion method and their electro catalytic activities were tested in Nuvant systems. Some of the catalyst characteristics are presented in Table 2.

XRD patterns obtained for example for LaRuO₃ and LaRuO₃-Pt catalyst, as well as Pt-black are shown in Figure 1. It can be seen that crystallinity of the perovskite powder is slightly higher than of those diluted with platinum. This effect can be explained by lower reaction temperature of the perovskite/Pt system as compared to pure perovskite. It is interesting that specific surface areas of the oxide powders are typically higher than for oxide-metal composition (see Table 2). The latter is related to the larger amount of gas-phase products during combustion of non diluted solutions [17]. Comparison of different XRD patterns also allows to conclude that platinum exists in the composite catalyst as a separate phase. Indeed, on one hand, the Pt peaks were consistently detected on the samples where metal was added (Fig. 1). On the other hand, no quantifiable changes of perovskite peaks position were observed, which could indicate that metal incorporated into perovskite structure. Qualitatively similar trends were obtained for the other perovskite materials (*i.e.* BaRuO₃, CaRuO₃, SrRuO₃, SrFeO₃).

The data on the specific surface (S) and loadings of some catalysts are summarized in Table 2. One trend may be outlined, *i.e.* the nitrates with lower phase transformation temperatures (melting, boiling, decomposition) lead to higher surface area of the synthesized products. For further discussion it is also important that S of the standard catalysts (*i.e.* Pt-Ru and Pt-black) are higher as compared to the synthesized materials. Also note that amount of platinum in perovskite-metal composite is ~ 10 times less that in Pt-Ru standard.

Electro-catalytic Activity

Typical polarization curves obtained at sweeping rate of 20 mV/s for synthesized compositions are presented in Fig. 2. It can be seen that all ARuO₃ perovskites (curves 1-4) show considerable current densities with an onset potential around 0.3 V, while
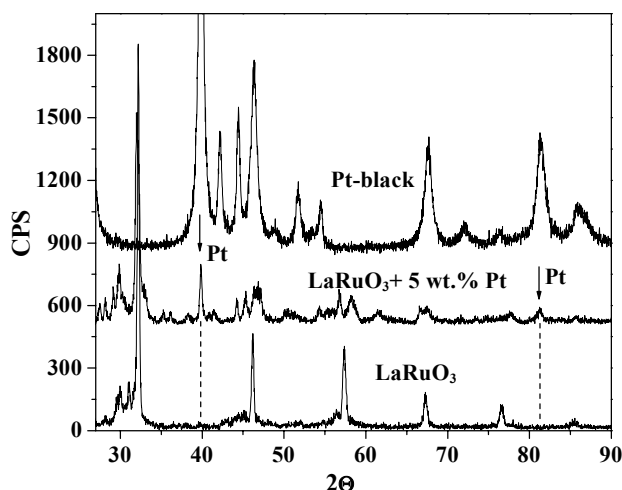
Fig. 1. XRD patterns of LaRuO₃, LaRuO₃ + 5wt.% Pt and Pt-black catalyst.

very small activity was observed for SrFeO₃ compositions (*e.g.* curve 5 for SrFeO₃). This result suggests that Ru element in the perovskite structure plays a significant role in the considered electro-catalytic process. It is well known that during electro-oxidation of alcohols on Pt-Ru catalyst, ruthenium activates water and provides preferential sites for OH group adsorption at low potential [28,29]. These OH groups are essential for complete oxidation (to CO_2) of the intermediate chemisorbed species. Thus it was demonstrated that not only SrRuO₃, as it was shown in our previous work [24], but many other mixed-conductor complex perovskites with ruthenium on B-site can be a promising base for development of the effective catalysts for DEFC.
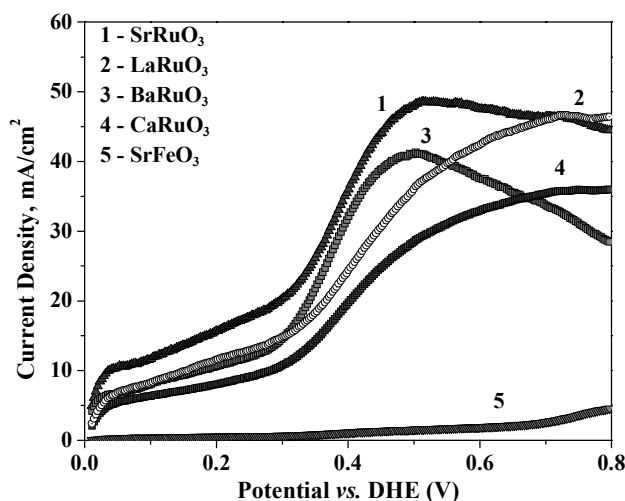
Fig. 2. Voltammograms for different perovskite electrodes at a sweep rate of 20 mV/s, temperature of 80°C and ethanol flow rate of 8 ml/min.

It is also interesting that having higher specific surface area (see Table 2) $CaRuO_3$ shows lower activity as compared to other perovskites. This result indicates the important role of A-site ion in the process of ethanol oxidation. In addition, a close inspection of Fig. 2 reveals that perovskites with Sr (curve 1) and La (curve 2) on A-site show the higher electro-oxidation activity as compared to Ca and Ba based materials. More important that while $SrRuO_3$ and $LaRuO_3$ stand out with the best performance in terms of current density, their voltammograms are qualitatively different. The Sr-based perovskite exhibits a maximum ("hump") in current density at potential ~ 0.5 V. Same "strange" behavior was observed for this catalyst during oxidation of the methanol [24]. However, $LaRuO_3$ catalyst possesses monotonic increase of current with density in the investigated (0-0.8 V) voltage range. It is still not clear if it is related to the fact that Sr is an alkali earth element and La is a rare earth element. La and Sr-based perovskites were selected as a basis for the below we focus on more detailed characterization of these two most promising compositions.

Figure 3 shows oxidation performance for $SrRuO_3$ and $LaRuO_3$ catalysts as a function of temperature. As could be expected the maximum current density for both catalyst drops as temperature decreases, indicating that the electro-catalytic reaction is a thermally activated process. However, the current maximum of the first peak (more pronounced for $SrRuO_3$; Fig. 3a), which appears at potential ~ 0.1 V, increases as temperature decreases. This behavior suggests that this peak is probably is related to the adsorption processes (see also [27]).
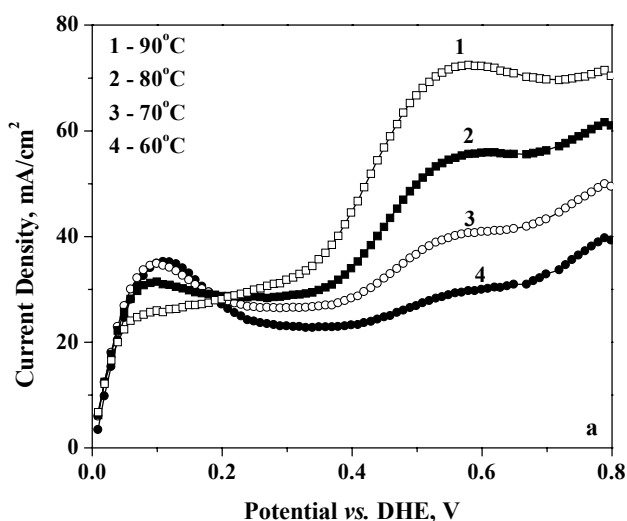
While pure perovskite catalysts show relatively high oxidation activity, the observed current values are lower than for Pt-based alloy (compare curves 1-3 in Figure 4). Thus next step in multifunctional catalyst design involved preparation of perovskite-platinum composite. In previous work [24] we used two approaches for Pt incorporation into oxide-based catalyst, *i.e.* "internally" during solution combustion (SC) synthesis or "externally" during ink preparation. It was shown that internal method, where complex-catalysts were synthesized by addition of Pt containing reagent (*e.g.* tetra-ammine-platinum nitrate) into initial metal nitrate + glycine solution, leads to superior electro-catalytic activity of produced compositions. Thus all results discussed below were obtained on oxide-metal catalysts synthesized by internal SC method.

Figure 4 (a) presents the comparison of linear scan voltammetry (polarization curves) of ethanol oxidation for perovskite-based and standard Pt-based catalysts. It can be seen that in terms of current density, the composite perovskite-Pt (curve 4) catalyst substantially outperform both the pure $SrRuO_3$ (curve 3) and standard Pt-black (curve 2) catalysts, and is comparable with the characteristics of the Pt-Ru alloy (curve 1). Moreover, the data on current densities for different catalysts normalized by Pt loading (Fig. 3b) clearly show that perovskite based composite (curve 3) is the most effective. For example, $SrRuO_3 + 5$ wt.% Pt catalyst is better than Pt-Ru alloy by a factor up to 4. Similar trend was observed for $LaRuO_3$-based catalysts (*e.g.* see Fig. 5).
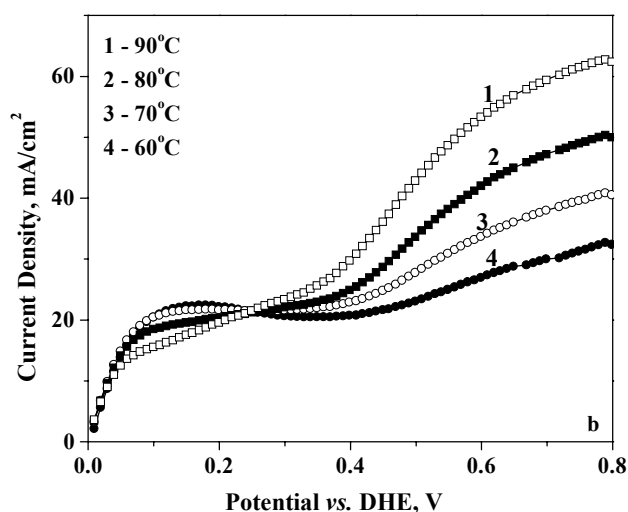
Fig. 3. Voltammograms for (a) $SrRuO_3$ and (b) $LaRuO_3$ electrodes as a function of temperature obtained at a potential sweep rate of 20 mV/s and in 1.0M CH_3CH_2OH with flow rate of 8 ml/min.
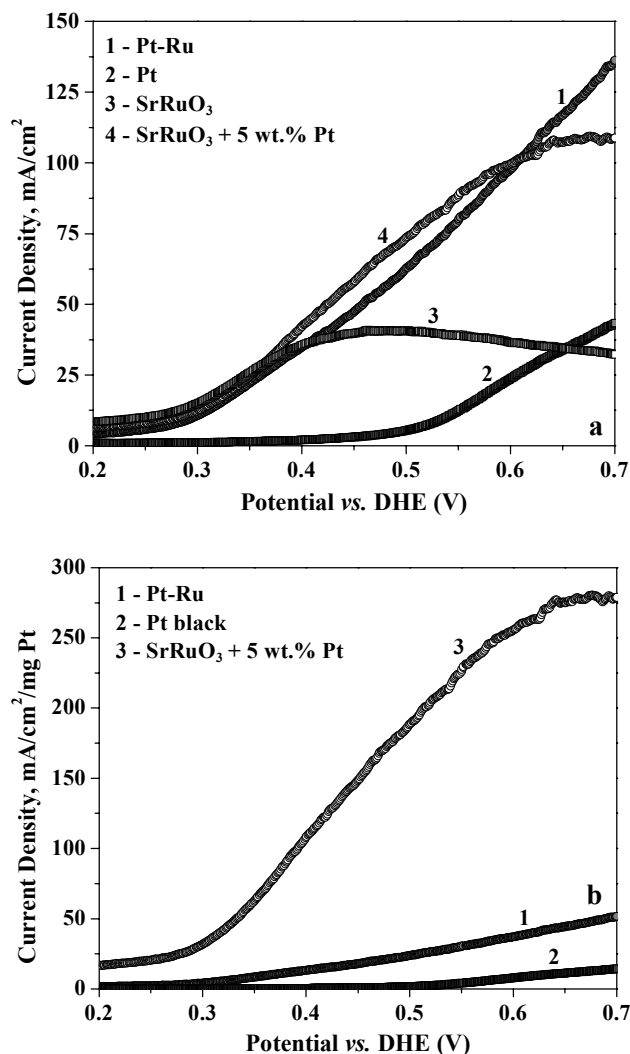
Fig. 4. Comparison of ethanol oxidation performance for SrRuO$_3$-based and standard Pt-based catalysts: (a) original data; (b) data normalized on Pt loading (Conditions: 1M ethanol, flow rate 8 ml/min, potential sweep rate 2 mV/s, temperature 90°C).

Fig. 5. Comparison of ethanol oxidation performance for LuRuO$_3$-based and standard Pt-based catalysts: (a) original data; (b) data normalized on Pt loading (Conditions: 1M ethanol, flow rate 8 ml/min, potential sweep rate 20 mV/s, temperature 90°C).

On one hand, these result (Fig. 4a and 5a) supported previously obtained data [24] on effectiveness of the preparation of the composite oxide/Pt catalyst by "internal" combustion synthesis approach. On the other hand, it is illustrated (4b and 5b) that catalytic activity of Pt can be significantly enhanced by metal embedding in the Ru-contained perovskite structures. It is important to outline that because specific surface areas of the composite catalysts (~ 7 m^2/g) are lower as compared to Pt-Ru standard (~ 65 m^2/g) and amount of Pt is also more than 10 times lower (see Table 2), the observed effect can be related to: (i) the high activity of platinum sides distributed along the perovskite surface during solution combustion synthesis; (ii) the active role of perovskite constituent.

Admitting that shown above and used in our previous work [24] potential sweep approach has some limitations related to the relatively high scanning rates, in this work potentiostatic measurements were also conducted at different *constant* potentials in the range 0.1-0.7 V. Figure 6a shows example of such current-time transients recorded for perovskite-based and standard Pt-based catalysts at a constant anode potential of 0.6 V (potential prior to the step = 0.05 V). Note that duration of the current measurements were long enough (order of several minutes) to reach some kind of current saturation.

To understand these results one has to account that in the response to a potential step, the total measured current, i_T, involves at least three components:

faradaic current i_F, the charging current i_C, both decaying with time t, and a noise current: $i_T = i_F + i_C + noise$. As i_C decays exponentially, after a short period (several seconds) the current becomes predominantly of faradaic nature, approaching a steady state value. The observation of appreciable current density value for SrRuO$_3$ (curve 3) at 0.6 V confirmed its reasonable electrocatalytic activity for ethanol oxidation. It is more important that observed steady current density value for perovskite-Pt composites (curves 4 and 5) are essentially similar to Pt-Ru alloy catalyst (curve 1). Interesting that same measurements for SrRuO$_3$ catalyst conducted for methanol oxidation shows significantly lower i_F current (see curve 6, Fig. 6).

The plots of current densities versus applied potential for these catalysts grabbed at different sampling times (*e.g.* 5 and 100 seconds) are presented in Figs. 5(b) and (c). Apparently, the SrRuO$_3$-Pt catalyst shows a comparable performance with Pt-Ru in potential range (0.4-0.7 V). It is also noteworthy that drop of current with time for perovskite-metal catalyst is insignificant. For example, at $V = 0.6$ V, current density decreases for SrRuO$_3$-Pt catalyst by a factor of only 1.4. The latter result could imply that such catalysts could deliver stable performance in real fuel cell systems.

Conclusions

In this paper for the first time it is demonstrated the series of mixed-conductor perovskites could be effective phases for development of the active and cheap catalyst for the direct ethanol fuel cells. Also it was shown that LaRuO$_3$ possessing similar activity with previously reported SrRuO$_3$ composition, does not perform "hump" type (with maximum) behavior [17], but its *I-V* curve has a monotonic character. Comparison of the different catalysts specific surface areas and Pt loadings allowed us to conclude that observed effects of high activity for oxide/Pt composites are related to the higher activity of Pt-sites deposited on the perovskite basis during solution combustion synthesis of the catalysts and. Simultaneously it is shown that role of the chemical nature of the oxide constituent is very important. The optimizations of (i) perovskite composition (by doping from A and B sites), and (ii) Pt loading are currently under investigations.

The above findings undoubtedly show that suggested approach for design of multifunctional cata-
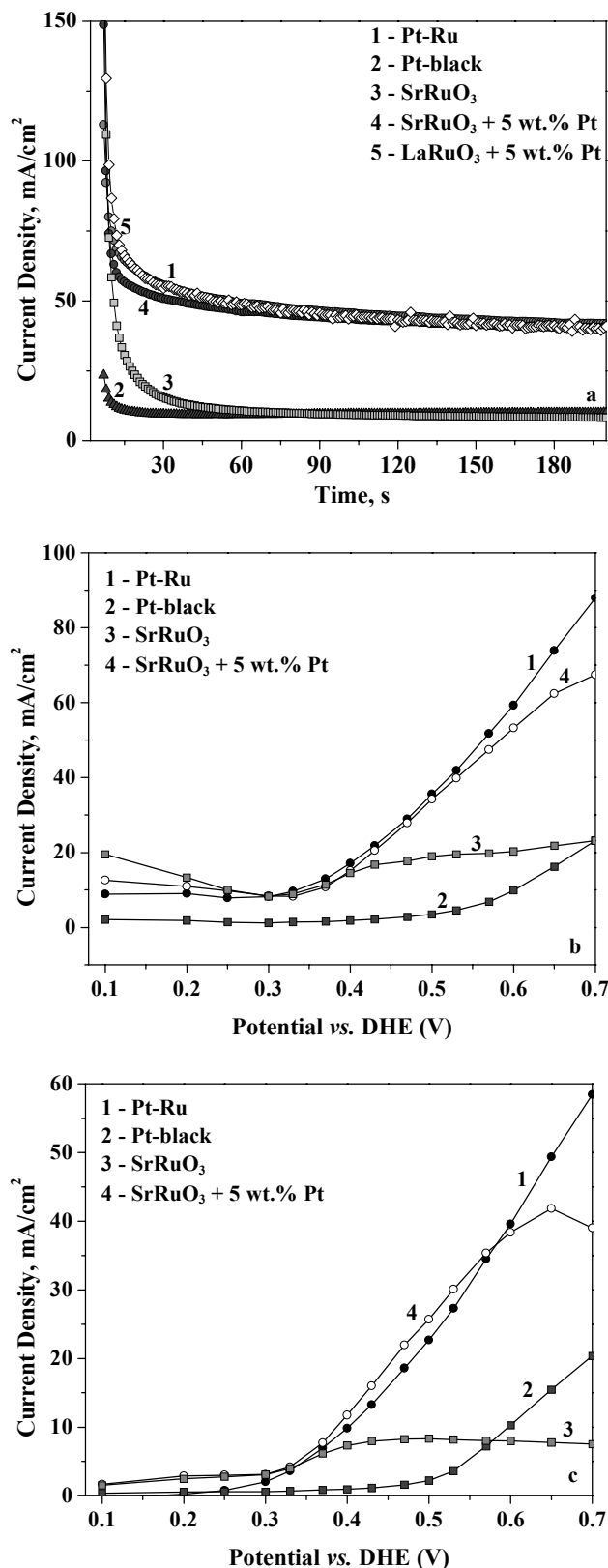
Fig. 6. (a) The potential step results at $V = 0.6$ V for perovskite-based and standard Pt-based catalysts; (b),(c) corresponding current density-potential plots for different sampling time, t: (b) $t = 5$ s, (c) $t = 100$ s (Conditions: 1M ethanol, flow rate 8 ml/min, temperature 60°C).

lyst is effective. This encouraging result suggests that such multifunctional catalysts prepared by combustion technique may hold a key for cost friendly solution of effective DEFC design.

Acknowledgement

References

1. Dircks, K. Recent Advances in Fuel Cells for Transportation Application, EVS15, Brussels (Belgique), October 1998.
2. Lamy C.; Lima, A.; LeRhun, V.; Delime, F.; Coutanceau C.; Léger, J.-M. J. Power Sources 2002 105, 283.
3. Lamy, C.; Belgsir, E. M.; Léger, J.-M. J. Appl. Electrochem. 2001 31, 799.
4. Baldauf, M.; Preidel, W. J. Power Sources 1999 84, 161.
5. Lamy, C.; Rousseau, S.; Belgsir, E.M.; Coutanceau, C.; Léger, J.-M. Electrochimica Acta 2004 49, 3901.
6. Perez, J. M.; Beden, B.; Hahn, F.; Aldaz, A.; Lamy, C. J. Electroanal. Chem. 1989 262, 251.
7. Hitmi, H.; Beligsir, E. M.; Léger, J.-M.; Lamy, C.; Lezna, R. O. Electrochimica Acta 1994 39, 407.
8. Fujiwara, N.; Friedrich K. A.; Stimming, U. J. Electroanal. Chem. 1999 472, 120.
9. Song, S. Q.; Zhou,W. J.; Zhou, Z. H.; Jiang, L. H.; Sun, G. Q.; Xin, Q.; Leontidis, V.; Kontou, S.; Tsiakaras, P. Int. J. Hydrogen Energy 2005 30, 995.
10. Zhou, W. J.; Song, S.Q.; Li, W.Z.; Sun, G.Q.; Xin, Q.; Koutou, S.; Poulianitis, K.; Tsiakaras, P. Solid State Ionics 2004 175, 797.
11. Delime, F.; Léger, J.-M.; Lamy, C. J. Appl. Electrochem 1999 29, 1249.
12. Vigier, F.; Coutanceau, C.; Perrard, A.; Belgsir, E. M.; Lamy, C. J. Appl. Electrochem 2004 34, 439.
13. Pena, M. A.; Fierro, J. L. G. Chem. Rev. 2001 101, 1981.
14. Norby, T. Solid State Ion. 1999 125, 1.
15. Deshpande, K.; Mukasyan, A.S.; Varma, A. Chem. Mater. 2004 16, 4896.
16. Varma, A.; Mukasyan A.S.; Deshpande K.; Pranda P.; Erii, P. Mat. Res. Soc. Symp. Proc. 2003 800, 113.
17. Deshpande, K.; Mukasyan, A.S.; Varma, A. J. Am. Ceram. Soc. 2003 86, 1149.
18. Liu, R.; Smotkin, E. S. J. Electroanal. Chem. 2002 535, 49.
19. Diaz-Morales, R. R.; Liu, R.; Fachini, E.; Chen, G.; Segre, C. U.; Marinez, A.; Cabrera, C.; Smotkin, E. S. Journal of the Electrochemical Society 2004 151, A1314.
20. Patil, K.C.; Aruna, S.; Mimami, T; Curr. Opin. Sol. State Mater. Sci. 2002 6, 507.
21. Rao, G.R.; Sahu, H.R.; Mishra, B.G. Colloids Surf. A., 2003 220, 261.
22. Hwang, C.; Wu, T. J. Mater. Sci. 2004 39, 6111.
23. Dinka P.; Mukasyan A.S., J. Phys. Chem. 2005 109(46), 21627.
24. Deshpande, K.; Mukasyan, A.S.; Varma, A. J. Power Sources, 2006 158(1), 60.
25. Mukasyan, A.S.; Epstein P.; Dinka, P., Proceed. Combust. Institute, 2007 31(2) 1789.
26. Wilson, M.S.; Gottesfield, S. J. Appl. Elecrochem. 1992 22, 1.
27. Goodenough, J. B. Localized to Itinerant Electronic Transition in Perovskite Oxides, 2001, 19.
28. Watanbe, M.; Motoo, S. J. Electroanal. Chem. 1975 60, 267.
29. Kabbabi, A.; Faure, R.; Durand, R.; Beden, B.; Hahn, F.; Léger, J.-M., Lamy, C. J. Electroanal. Chem. 1998 444, 41.